ISSN 1027-5495. Functional Materials, 27, No.3 (2020), p. 567-574.
doi:https://doi.org/10.15407/fm27.03.567 

# Modeling of a diffraction pattern from light-induced gratings in AgCl–Ag waveguide film as a method of evaluation of the grating parameters

***Ye.D.Makovetskyi***

Physical Optics Chair, V.Karazin Kharkiv National University,
4 Svobody sq., 61022 Kharkiv, Ukraine

*Received December 12, 2019*

Modeling of evolution of a diffraction pattern under action of a laser beam on a composite waveguide AgCl–Ag film has been performed for the first time; a 100 nm thick film was used as an example. Visual structures of calculated and experimental patterns are similar both in separate moments and in dynamics (videos were compared). This is a confirmation of validity of current understanding of the mechanism of development of diffraction gratings induced in AgCl–Ag film. During the simulation, the possibility of refining the grating parameters was demonstrated; this is based on the similarity of the diffraction patterns as a whole, and not just their individual reflections. The mean value obtained for angular dispersion of grating vectors unambiguously proves the domain nature inherent in the aggregate of the gratings.

**Keywords**: light-sensitive film, waveguide film, diffraction grating, diffraction pattern, modeling.

**Моделювання картини дифракції від світлоіндукованих граток у хвилеводній плівці AgCl–Ag як спосіб оцінювання параметрів гратки**. *Є.Д.Маковецький*

Вперше проведено моделювання еволюції картини дифракції лазерного пучка від композитної хвилеводної плівки AgCl–Ag на прикладі плівки товщиною 100 нм. Візуальні структури обчислених та експериментальних картин є аналогічними як в окремі моменти часу, так і у динаміці (порівнювалися відео). Це є підтвердженням існуючих уявлень щодо механізму розвитку у плівці AgCl–Ag індукованих дифракційних граток. Показано можливість уточнення параметрів граток у ході моделювання, яке базується на відповідності експерименту дифракційної картини у цілому, а не тільки її окремих рефлексів. Отримане середнє значення кутового розкиду векторів граток доказує, що сукупність граток у плівці має принципово доменний характер.

Впервые проведено моделирование эволюции картины дифракции лазерного пучка от композитной волноводной плёнки AgCl–Ag на примере плёнки толщиной 100 нм. Визуальные структуры расчётных и экспериментальных картин аналогичны как в отдельные моменты времени, так и в динамике (сравнивались видео). Это является подтверждением существующих представлений о механизме развития в плёнке AgCl–Ag индуцированных дифракционных решёток. Показана возможность уточнения параметров решёток в ходе моделирования, которое основывается на соответствии эксперименту дифракционной картины в целом, а не только её отдельных рефлексов. Полученное среднее значение углового разброса векторов решёток доказывает, что совокупность решёток в плёнке имеет принципиально доменный характер.

## 1. Introduction

A number of nonlinear optical effects have been discovered using lasers due to their higher available power and due to smaller spread of beam parameters than those provided by spontaneous radiation sources. These effects include the effect of inducing diffraction gratings (DGs) by an interference field created by the superposition of the laser beam and scattered radiation. Initially the effect was discovered on surfaces of solids as a side effect of laser drilling [1]. Later, a similar effect was discovered in waveguide films of silver halides exposed to low-power laser beams (see the review [2]).

Because of the low power of scattered radiation, the medium must be able to memorize the previous effect in order to ensure a cumulative nature of the changes in the medium. Therefore, Kerr media are not suitable for manifestation of the effect, as nonlinearities of their responses are caused only by the nonlinearities of deviations of atom nuclei and electrons from their equilibrium positions. When illumination is terminated, atoms of the Kerr medium revert to their equilibrium states immediately.

Accumulation of changes in such media as photorefractive crystals (PC) is provided by ionization of atoms happened to be within brighter regions of the interference field, and by capturing the charges (electrons or holes) by traps within darker regions [3]. Macroscopic charge redistribution within the periodic or quasiperiodic interference field creates corresponding distortions of the PC lattice, thus creating phase or amplitude-phase DGs. Beam shutdown does not destroy the accumulated changes in the PC. As long as traps' energy depths substantially exceed kT value, both charge distribution and lattice deformation are preserved until the crystal gets illuminated again.

AgCl–Ag waveguide films were studied in this paper; specifically, the polycrystalline AgCl films with excessive granular silver. Such films are created by consecutive thermal vacuum deposition of AgCl and Ag onto surfaces of transparent solids. Memorizing the parameters of the illuminating beam is even more pronounced in these films than in PC. Similar to PC, electrons leave illuminated regions (here because of photoelectric effect on Ag granules) and get captured by traps in darker regions of the interference field. In this case, the field is created by the laser beam and scattered waveguide modes with diversely directed β vectors. The rest of scattered waves either quickly leaves the film or quickly dissipates due to destructive interference. Another difference from PC is a high ionic conductivity of these polycrystalline films. This allows the $Ag^+$ ions to be displaced, and the static electric field of trapped electrons results in moving the ions to the dark areas where they recombine. Thus, the displacement of silver ions to the minima of the interference pattern creates a phase-amplitude DG with grooves of granular silver. An important feature of the medium response is the positive feedback in the DG growth: diffraction of the laser beam by the DG amplifies the mode in which the DG was created. This leads to an increase in the contrast of the interference pattern, thus increasing the DG diffraction efficiency, and so on.

Exponential growth of DGs is hampered by two factors. Firstly, the irradiated area and the mass of involved silver are limited resources while there is competition of many gratings. The DGs grow in different directions from a number of scattering centers which are both AgCl layer defects and silver granules. As a result of simultaneous developing of the many adjacent gratings within the illuminated area of the film, the developing structure has a domain character [2]. Secondly, there is permanent change in the value of the film's effective refractive index *neff* which determines the value of mode propagation constant β. For a composite film with a small filling factor by colloidal particles (as in the case for AgCl–Ag films used here) $n_{eff}$ is calculated using the Maxwell-Garnett formula [4]. The reason of changing $n_{eff}$ is termination of interaction of silver atoms with light as the atoms migrate to dark areas of the interference field. Since the change of $n_{eff}$ value changes the value of β, the period of the interference pattern $d$ also changes. The simplest formula is for normal beam incidence: $d = 2\pi/\beta$. The change in $d$ value results in redistribution of silver atoms to conform to the new interference pattern, but since the attempt of atoms to get into the dark region itself changes the $n_{eff}$ value and changes location of the dark regions, the process goes on and on.

It is also important that indicatrix of initial scattered modes is sensitive to such beam parameters as the angle of incidence and state of polarization, e.g. see [5]. So, due to complexity of the DG evolution process, a rigorous mathematical model has not yet been developed, despite the many results

on the development of DG with a reasonable qualitative and semi-quantitative explanation of the experimental results. In this paper, for the first time, a quantitative model of evolution of the diffraction pattern is developed on the basis of the Monte Carlo method. Comparison of the calculated temporal evolution of the diffraction patterns with the video recording of the evolving experimental pattern provides new opportunities for estimating the parameters of the DG development.

## 2. Experimental

The AgCl–Ag polycrystalline films were deposited onto glass substrates by sequential thermal evaporation of AgCl and Ag in a vacuum of $10^{-5}$ mm Hg using a VUP-5M vacuum post. The thickness of the AgCl layer was $h = 100$ nm, the mass thickness of the granular Ag layer was 10 nm. These samples were illuminated according to the scheme of Fig. 1 using a linearly polarized semiconductor laser beam with wavelength of $\lambda = 650$ nm and power of $P = 25$ mW. The beam was focused on the film by a collecting lens with a focal length of $F = 8.5$ cm. The illumination was carried out along the normal to the samples. The so-called small-angle scattering (SAS) pattern was observed on a screen put across the beam immediately after the lens, at a distance of $R = 8$ cm from the sample. The screen had an aperture for the laser beam to pass through.

Despite the established name, the SAS pattern is a pattern of diffraction of waveguide modes propagating through DGs in the film. A SAS pattern can be observed in the transmitted light as well. In the case of oblique incidence, there are even four spatial angle regions where the SAS pattern exists, around four directions: along and against the original laser beam; along and against the beam reflected from the sample. The choice of screen location as in Fig. 1 was made to simplify experiments with off-normal incident beams, since there is no need to shift the screen when the angle of incidence changes.

Provided that the AgCl film thickness is 100 nm and the refractive indices are $n_{AgCl} = 2.06$ and $n_S = 1.515$ (a glass substrate), only $TE_0$ and $TM_0$ waveguide modes can propagate in the film. The combination of normal beam incidence and a linear polarization leads to the simplest form of the SAS pattern: to the scattering and diffraction band from DGs on $TE_0$ modes along the polarization plane without beam focusing [2], or to the so-called "torch" in SAS if the beam is focused on the film [6]. The torch is an aggregate of a large number of light speckles, and it is stretched along the polarization plane. The speckles appear, shift, split, merge and vanish within the torch region, thus reflecting the restructuring of DGs in the film in real time. Under normal beam incidence, $TM_0$ modes do not create DGs, since their initial scattering intensities are too small [7]. A video of the SAS torch evolution was recorded during illumination (see frames in Fig. 2). The bright horizontal line in the middle of each picture is a video artifact caused by the high brightness of the aperture area in the central part of the picture due to scattering on the edges of the screen aperture. The laser beam image is superimposed on the bright line, from the aperture to the left side of the picture.

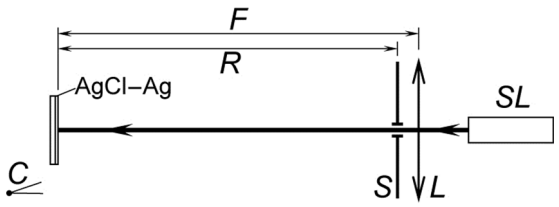


Fig. 1. Scheme of the experiment, view from above. The linearly polarized beam of a semiconductor laser (SL, $\lambda = 650$ nm, $P = 25$ mW) was focused on the surface of AgCl–Ag film by the lens $L$ with focal distance $F = 8.5$ cm. The screen $S$ with an aperture was placed at the distance $R = 8$ cm from the illuminated film. Diffraction patterns on the screen were recorded with a camera placed at $C$ point.

The focusing provides four features of DG development which influence the SAS patterns. Firstly, the irradiated spot area is decreased multiple times (to approximately 25 $\mu m^2$ in our case) which leads to a decrease in the total number of DGs developing within the spot. Therefore the number of diffraction speckles in the torch is also decreased. Secondly, shrinking of spot dimensions results in reduction of the number of grooves per DG because DGs do not expand beyond the interference region. The smaller number of the grooves means the DG becomes even farther from an ideal infinite grating, so the angular spread of diffraction beams increases, and speckles become larger. Third, an increase in the energy flux through a unit of the DG area results in an increase of mode intensities, and diffraction speckles become brighter. Fourth, the same reason leads to accelera-

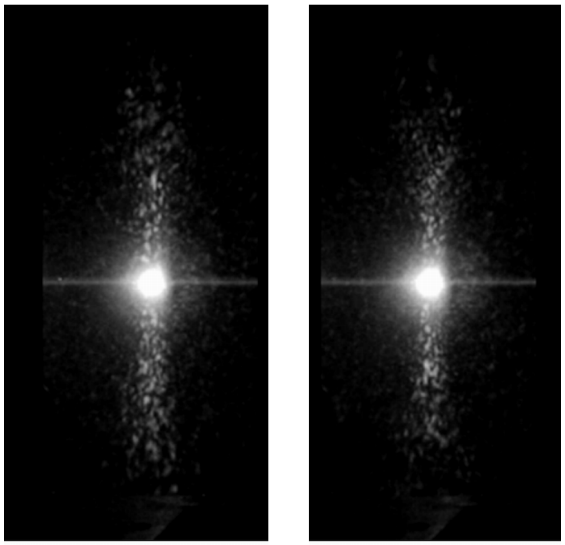


Fig. 2. Diffraction patterns on the screen $S$ in Fig. 1. Beam polarization plane is vertical. (a) A frame after 2 seconds of illumination; (b) after 10 sec. The screen aperture is in the center. The vertical set of changing light speckles is the "torch" modeled in this work.

tion of speckle movement in the torch due to dependence of this cumulative effect on the exposure time [8].

The lens with $F = 8.5$ cm has a sufficient optical power so that the SAS pattern splits into speckles due to the above factors. But its power is not as large as needed to turn the speckle movement into undecipherable flickering. So the SAS pattern under such conditions had been chosen for modeling.

### 3. Modeling

When the described AgCl–Ag films are illuminated, initial waveguide modes are excited by scattering on film defects. The quasiperiodic interference field of these scattered modes and the beam causes a quasiperiodic modulation of Ag concentration, thus DGs appear. After that, scattering by a periodically ordered ensemble of Ag particles should be treated as diffraction. The initial stage of scattering by disorganized particles was not modeled in this work since SAS torch is developed only during the diffraction stage. But the initial indicatrix of scattering of the waveguide modes imprints itself on the distribution of the DG vectors.

In all the calculations and in experimental patterns in Fig. 2, the center of the aperture in the screen was considered to be the origin of screen coordinates, the $x$ and $y$ axes on the screen plane were directed to the right and up, the $k_x$ and $k_y$ axes on the film plane were defined similarly with coordinates measured from the center of the illuminated region. At normal incidence, $k_x$ and $k_y$ axes coincide with $x$ and $y$ axes. In all the calculations, the third dimension of the film was disregarded, since film thickness of 100 nm is approximately four times less than even a single DG period [2]. Let $\alpha$ be the azimuth angle measured from $k_x$ axis in the $(k_x, k_y)$ plane.

As it is known [9], the scattering intensity of a beam linearly polarized along $k_y$ on small particles (much smaller than the wavelength) is determined by the law

$$I \sim \cos^2\alpha, \qquad (1)$$

which determines also relative intensities of initially scattered TE-modes. The vectors $\boldsymbol{K}$ of the gratings created by interference of each mode (with its $\beta$ vector) and an obliquely incident beam are determined by the formula

$$\boldsymbol{K} = \beta - \boldsymbol{k}_x, \qquad (2)$$

where $\boldsymbol{k}_x$ is the component of the beam wave vector $\boldsymbol{k}$ along the intersection of the incidence plane and the AgCl–Ag film plane. Diffraction of the beam with $\boldsymbol{k}_x$ of the order $m = 1$ on the grating with $\boldsymbol{K}$ leads to excitation of the same mode $\beta$ as the one which created the grating. This situation is called the stimulated Wood anomaly [10]. It promotes growth of each DG by channeling beam energy into waveguide modes.

Zeroing the angle of incidence simplifies the situation by eliminating the dependence of $\boldsymbol{K}$ magnitude on $\beta$ direction, and also provides amplification of modes with vectors opposite to each $\beta$ because the diffraction order $m = -1$ also creates waveguide modes. This is the so-called double Wood anomaly [7]. Under such conditions, DGs are known to develop with $\boldsymbol{K}$ vectors having azimuths $\alpha$ within $\pm 20°$ from $0°$ or $180°$ [2]. Neighboring DGs with close $\boldsymbol{K}$ merge into a single DG. Lengths of $\beta$ and $\boldsymbol{K}$ have a spread, and illuminating the film by red light reduces the lengths with time due to decreasing $n_{eff}$ of the film in which an increasing portion of Ag is concentrated in the minima of interference [8]. At the initial stage of illumination, the value of $n_{eff}$ exceeds 2.3 [2]. Eventually, when all the silver is piled up in dark areas of interference, $n_{eff}$ should reach $n_{AgCl} = 2.06$. The

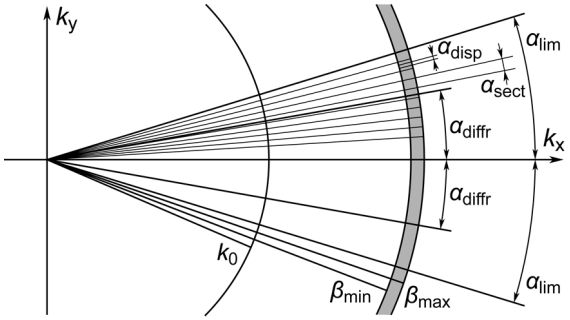


Fig. 3. The scheme of creating the multitude of vectors $\boldsymbol{K}$ of modes which form the gratings. It is shown in the reciprocal space of wave vectors. Each vector starts at the origin of coordinates and ends at a random point within a "cell" assigned to it between allowable β values (the gray ring between $\beta_{min}$ and $\beta_{max}$) and edges of the $\alpha_{sect}$ sector allocated to this grating within $\pm\alpha_{lim}$ (and within $180^{\circ}\pm\alpha_{lim}$ too, not shown here). The angles $\alpha_{diffr}$ and $\alpha_{disp}$ are also shown here. The former one limits diffraction while the latter angle is the characteristic angular dispersion of gratings' vectors.

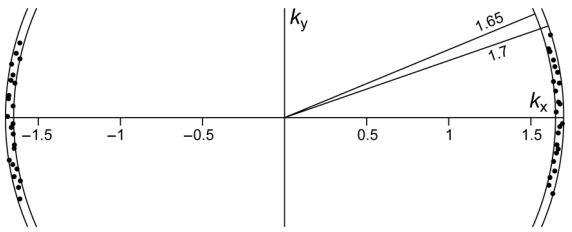


Fig. 4. An example of a set of diffraction grating vectors $\boldsymbol{K}$ (frame No. 4 of calculated evolution) is shown as the set of endpoints of the vectors starting from the origin of coordinates in the reciprocal space of wave vectors ($k_x$, $k_y$). The numbers are in $k$ units (wavenumber of the laser beam in vacuum).

$n_{eff}$ value decreases with different speeds at the center and on the periphery of the illuminated area due to different power in central and peripheral parts of the beam [8]. The periphery was not taken into account in this simulation, since its small contribution to the diffraction pattern may be ignored.

The SAS patterns appear due to Bragg diffraction of waveguide modes on DGs. Wave vector of the diffracted beam of $m$-th order is

$$\boldsymbol{k_d} = \boldsymbol{\beta_1} - m\boldsymbol{K_2}. \qquad (3)$$

The shape of the SAS depends on diffraction efficiencies of DGs and intensities of modes. The greater the distance on the screen from the coordinate origin to the diffraction speckle, the greater the difference between the vector $\boldsymbol{\beta_2}$ of the diffraction mode and the vector $\boldsymbol{\beta_1}$ of the mode that created the DG with $\boldsymbol{K_1}$ in accordance with (2). If only one DG has been developed and only its mode intensity is large, then diffracted beams propagate solely along the laser beam. The other extreme would be if all the DGs were developed with equal diffraction efficiencies, and the torch height on the screen would not be limited. If there were only two strong modes with β vectors lying in horizontal plane (where TE-mode scattering maxima are) but there were all possible DGs, or if there were all the modes, but DGs only with horizontal $K$ vectors, then instead of a torch there would be a pair of light arcs touching at the screen aperture, with a joint vertical tangent. The torch observed in the experiment (see Fig. 2) is far from these extremes, but their traces are noticeable.

The scheme of performed calculations was as follows. According to (1), azimuths α with TE-mode scattering intensity big enough to trigger the DG development are limited by $\pm\alpha_{lim}$ from 0° or 180°. The value of $\alpha_{lim}$ is adjustable and is less than 20°. These angle intervals are divided into smaller $\alpha_{sect}$ sectors (about 1°, also an adjustable parameter). Within each $\alpha_{sect}$, the development of only one DG is supposed to happen (see Fig. 3) on a mode with β length within the interval from $\beta_{min} = 1.65k$ to $\beta_{max} = 1.7k$. This is a typical interval for the given AgCl layer thickness at the beginning of illumination [11]. The diffraction efficiency of each DG is proportional to the scattering intensity for its azimuth. Specific values of the angles and lengths of the mode vectors within designated limits were produced by the pseudo-random number generator of the Maple mathematical package with which all the calculations were performed. Each initial $\boldsymbol{K}$ vector of DG in the calculated case of normal incidence is equal to the initial β vector of its mode, but the arrays containing β and $\boldsymbol{K}$ data are separate for two reasons. Firstly, the mechanism of changes in the film consists in the displacement of atoms, so rebuilding of DGs cannot be as quick as the change in mode characteristics. Secondly, in the future these calculations are to be extended to the case of oblique incidence, when β and $\boldsymbol{K}$

cannot possibly be equal, see (2). An example of an ensemble of DG vectors is shown in Fig. 4; each point indicates the end of a $\boldsymbol{K}$ vector starting at the origin of coordinates.

Next, all possible combinations of modes diffracting on the DG are automatically calculated. If a pair of a mode and DG provides a diffraction beam towards the screen, the position of the center of the diffracted beam is calculated, and the image of the light spot is added to the generated image of SAS. The whole SAS image has a height of 500 pixels comprising the image of the screen 15 cm high (from Fig. 2). A standard image of the generated light spot was used with brightness decreasing with the distance from its center by the Gaussian function with a half width of several pixels (diameter $D$ of the spot is also an adjustable parameter). Brightness of each spot is determined by the product of the intensity of the mode and the DG diffraction efficiency which is considered to be directly proportional to the scattered mode intensity from (1). To reduce computer time of the calculations, stretching of peripheral spots along the spot-aperture direction was neglected, because it noticeably affects only weak peripheral speckles. Overlapping of the spots in the calculated SAS pattern creates an aggregate of speckles of irregular shape, similar to the experimental pattern.

For subsequent SAS frames, there are changes in parameters to represent DG rebuilding process in the film: the mode vectors are shortened by $10^{-5}$ $k$ between adjacent frames, a small random azimuth offset is added to reflect interaction with neighboring DGs during the restructuring (0.05° per frame, direction of shifting of a particular DG is constant for several frames in a row). These parameter values were selected to match rates of pattern changes in the experimental video and in the calculated one (for 8 frames per second). See the calculated patterns in Fig. 5a, b.

Understandably, these calculated patterns are not ideal. Among noticeable differences there are borders of speckles (which are sharper in experimental Fig. 2) and absence of weaker light speckles beyond the modeled "torch". The former indicates the need for a more suitable function (not yet known) than a Gaussian function for better characterization of the form of individual diffraction spots. The latter is the result of neglecting diffraction from periphery of the illuminated area. But neither of them hampers analyzing the DG development by torch speckles.

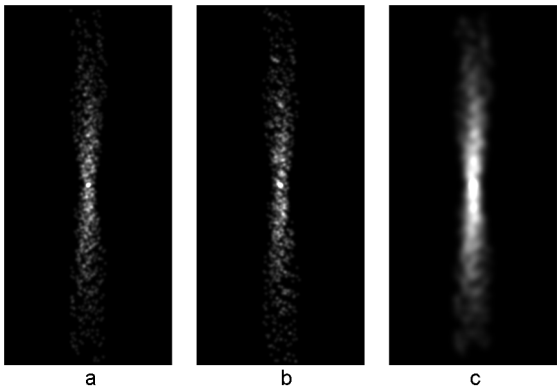


Fig. 5. Examples of diffraction patterns calculated for normal incidence of a vertically polarized beam focused on AgCl–Ag film at $\alpha_{sect} = 1.4°$. For diameter of each diffraction spot $D = 5$ pixels (i.e. $\alpha_{disp} \approx 0.5°$): (a) frame No. 4 (the pattern produced by gratings from Fig. 4); (b) frame No. 84. In (c) there is what happens to frame No. 4 if $D$ is increased to 14 pixels for $\alpha_{disp}$ to match the value of $\alpha_{sect}$.

## *4. Discussion*

Firstly, the fact of obtaining computed SAS patterns similar to experimental ones confirms the validity of present-day ideas about DG evolution in AgCl–Ag. Especially because of synergy: setting characteristics of individual modes and DGs (thus specifying individual diffraction reflections) provides a pattern with a regular torch made of randomly shaped moving speckles just as the experiment shows.

Secondly, new information on DG characteristics may be retrieved from the SAS patterns. For example, the mean value $\alpha_{disp}$ of angular dispersion of imperfect DGs' vectors which determines the angular width of diffraction beams. Consider the two following parameters which determine conformity of the pattern in Fig. 5a, b with the experimental one. The first parameter is the sector $\alpha_{sect}$ allocated for one DG in the reciprocal space of wave vectors. The second parameter is the diameter $D$ of the diffraction reflection on the screen. Assuming $\alpha_{disp}$ and $\alpha_{sect}$ to be equal, one assumes the values of $D$ and $\alpha_{sect}$ to be connected. But when $D$ is calculated on the basis of $\alpha_{sect}$ and the spread of the focused beam, the value of $D$ turns out to be too large, and the torch of too wide reflections turns into a solid white strip regardless of the selected values of $D$ and $\alpha_{sect}$. An example of such a pattern is provided in Fig. 5c. An attempt of reducing

$D$ by decreasing $\alpha_{sect}$ results in an increase of the number of reflections due to an increase in number of DGs which is determined by the number of $\alpha_{sect}$ sectors fitting within $\pm\alpha_{lim}$ and $180^\circ\pm\alpha_{lim}$ sectors. The area of each diffraction spot decreases in proportion to $D^2$, but the number of diffraction spots also increases quadratically, since the linearly increasing number of modes is multiplied by the linearly increasing number of DGs. The only way to achieve similarity of the calculated and experimental patterns is to abandon the assumption $\alpha_{disp} = \alpha_{sect}$. The patterns in Fig. 5a, b were calculated with selected values $\alpha_{sect} = 1.4^\circ$ and $D = 5$ pixels, the latter corresponding to $\alpha_{disp} \approx 0.5^\circ$ within each $\alpha_{sect}$. The frame No. 1 has the peculiarity of equal $\boldsymbol{\beta}$ and $\boldsymbol{K}$ vectors for each grating since it is the starting point of calculations; so in Fig. 5a, the frame No. 4 is shown. The value of $D$ is increased to 14 pixels in Fig. 5c while the rest of parameters are identical to Fig. 5a. The obvious mismatch of Fig. 5c pattern and experimental patterns Fig. 2 means that DG grooves cannot smoothly turn into grooves of other DGs throughout all the azimuth intervals of $\pm\alpha_{lim}$ or $180^\circ\pm\alpha_{lim}$. This means, the structure of DGs in AgCl–Ag film is domain-based in its nature, not because the author cut the DG into sectors like a cake and called each sector a separate DG. No microphotographic studies were carried out in this work; photographs can be seen e.g. in [2, 11]. But no matter how many DG photographs there are, they do not guarantee that there will be no DG grooves of the form of wide-angle arcs of concentric circles in the next photograph. But harmonization of the values of selected parameters in this modeling makes it feasible to say: that is impossible. If a structure of concentric grooves had arisen somehow, it would immediately split into separate competing domains; all of them exponentially develop until external factors impede them.

Thirdly, the modeling has revealed that previously observed difference between SAS patterns as a pair of touching arcs [12] and as a strip with no arcs [2] is caused by a restriction on possible cases of diffraction. According to (1), initial scattering provides modes predominantly along the directions close to the normal to the polarization plane, and diffraction of the external beam on DGs creates modes in the same directions. Thus, the DG domains develop elongated, and the length of each domain (along its $\boldsymbol{K}$ vector) is larger than the width of the domain (length of DG grooves), sometimes several times larger, more often several dozen times larger [11]. When diffraction (3) occurs with distinctly different directions of $\boldsymbol{\beta}_2$ and $\boldsymbol{K}_1$, the mode crosses the DG "transversely", and the interaction is scant. So the diffraction cases with great difference in azimuth angles may be disregarded. To produce a torch of the correct form, it is sufficient to limit the directions of diffracting modes to narrower angular ranges: $\alpha_{diffr} = 10^\circ$ (see Fig. 3) instead of $\alpha_{lim} = 16^\circ$. When the value of $\alpha_{diffr}$ is decreased, the central part of the torch (along the vertical polarization plane) shrinks faster than lateral sides; this fact is the basis of determination of the $\alpha_{diffr}$ value.

Despite the large number of parameters introduced, their values can be determined using the fact that they affect different aspects of the torch structure. The $\alpha_{lim}$ and $\alpha_{diffr}$ pair determines the vertical dimensions and shape of the torch (whether the arcs are pronounced or not). The difference between $\beta_{max}$ and $\beta_{min}$ determines the width of the torch along $x$ axis. The pair of $\alpha_{disp}$ and $\alpha_{sect}$ angles determines the "filling" of the torch with speckles.

## 5. Conclusions

In this work for the first time, the calculations have been performed to model the evolution of the small-angle scattering and diffraction pattern of a linearly polarized laser beam normally illuminating an AgCl–Ag composite waveguide film. The calculated patterns are similar to experimental ones both in statics and in dynamics. This is a confirmation of validity of current understanding of the mechanism of development of induced diffraction gratings in AgCl–Ag films. Adjustment of grating parameters in the course of modeling, while focusing on the pattern appearance in whole in accordance with the experiment, provided new information about the gratings. An important result is the proof that structure of the gratings is domain one, not because of random factors affecting initial scattering in the film, but due to inherent domain nature of the gratings.

Since the validity of the model has been confirmed in this work for the simplest illumination conditions (normal incidence and linear polarization of the beam), it is intended to carry out modeling of more complex cases. For example, oblique incidence of a laser beam introduces additional differ-

ences between the gratings with different mode azimuths: different periods, different modes (TE and TM), double Wood anomalies only for some gratings etc. Extensive experimental data on features of the grating development have been accumulated to date under various illumination conditions, and now there is a new computational tool for analyzing these results.

## *References*


1. A.M.Bonch-Bruevich, M.N.Libenson, V.S.Makin et al., *Opt. Engin.*, **31**, 718 (1992).
2. L.A.Ageev, V.K.Miloslavsky, *Opt. Engin.*, **34**, 960 (1995).
3. R.A.Rupp, F.W.Drees, *Appl. Phys.B*, **39**, 223 (1986).
4. V.K.Miloslavsky, L.A.Ageev, E.D.Makovetsky et al., *Functional Materials*, **15**, 313 (2008).
5. E.D.Makovetsky, V.K.Miloslavsky, L.A.Ageev, *J. Opt. A: Pure Appl. Opt.*, **7**, 324 (2005).
6. L.A.Ageev, V.K.Miloslavskii, E.I.Plavskaya, *Opt. Spectrosc.*, **88**, 916 (2000).
7. V.K.Miloslavsky, E.D.Makovetsky, L.A.Ageev, *Opt. Commun.*, **232**, 303 (2004).
8. V.I.Lymar, V.K.Miloslavskii, L.A.Ageev, *Opt. Spectrosc.*, **83**, 921 (1997).
9. C.F.Bohren, D.R.Huffman, Absorption and Scattering of Light by Small Particles, Wiley, New York (1983).
10. A.E.Siegman, P.M.Fauchet, *IEEE J. Quant. Electron.*, **22**, 1384 (1986).
11. L.A.Ageev, E.D.Makovetskii, V.K.Miloslavskii, *Opt. Spectrosc.*, **100**, 291 (2006).
12. L.A.Ageev, V.K.Miloslavsky, A.Nahal, *Pure Appl. Opt.*, **7**, L1 (1998).